

*lil*GYM: NATURAL LANGUAGE VISUAL REASONING WITH REINFORCEMENT LEARNING

Anne Wu, Kianté Brantley, Noriyuki Kojima, and Yoav Artzi

Department of Computer Science and Cornell Tech, Cornell University

{aw588, kdb82, nk654}@cornell.edu, {yoav}@cs.cornell.edu

ABSTRACT

We present *lil*Gym, a new benchmark for language-conditioned reinforcement learning in visual environments. *lil*Gym is based on 2,661 highly-compositional human-written natural language statements grounded in an interactive visual environment. We annotate all statements with executable Python programs representing their meaning to enable exact reward computation in every possible world state. Each statement is paired with multiple start states and reward functions to form thousands of distinct Markov Decision Processes of varying difficulty. We experiment with *lil*Gym with different models and learning regimes. Our results and analysis show that while existing methods are able to achieve non-trivial performance, *lil*Gym forms a challenging open problem. *lil*Gym is available at <https://lil.nlp.cornell.edu/lilgym/>.

1 INTRODUCTION

Reinforcement learning (RL) with natural language context poses important opportunities and challenges. Language provides an expressive and accessible conduit for task specification, so that RL agents can address a broad set of tasks, rather than learn a single behavior. For natural language processing (NLP), RL is a promising avenue for language use and acquisition with world interaction. However, language is a challenging medium to learn to reason about. It requires agents to reason about high-level language concepts, low-level actions, and the relations between them, and to learn to do so efficiently because language data is inherently limited due to requiring human interaction.

Despite significant interest and promising approaches, it has been challenging to create expressive RL benchmarks with natural language. A core challenge is accurately computing a reward that is dependent on natural language semantics. Existing approaches adopt different strategies to address this issue, such as using synthetic language (Côté et al., 2018; Co-Reyes et al., 2019) or heuristic approximation, for example via demonstration data (Misra et al., 2017). While these approaches open new avenues for research, they either do not explore the full complexity of natural language or introduce unexpected artifacts into learning through meaning approximations.

We present *lil*Gym,¹ a reinforcement learning benchmark for natural language visual reasoning that addresses the above issues. *lil*Gym implements the standard OpenAI Gym API (Brockman et al., 2016), and aims to bring natural language into the suite of commonly used RL benchmarks.

*lil*Gym is focused on spatial reasoning, with an agent that manipulates a visual environment by adding and removing objects conditioned on a natural language statement. The agent’s goal is to modify the environment so that a given statement will have a pre-specified truth-value with regard to the environment (i.e., the constraints specified in the language are either satisfied or violated). *lil*Gym includes 2,661 highly-compositional and semantically-diverse natural language statements and visual environment from the NLVR corpus (Suhr et al., 2017), that combine with a configurable environment backbone to create thousands of Markov Decision Processes (MDP) of varying complexity, for example with different sizes of the state and action spaces.

A key challenge in constructing *lil*Gym is accurate reward computation. Because of the flexibility of the environments and language, there are many possible equally correct termination states for

¹*lil*Gym stands for Language, Interaction, and Learning Gym.

each MDP. Correctly evaluating reward at every possible state requires taking into account the semantic nuances of the highly-compositional language. We address this problem by annotating all statements with executable Python programs representing their meaning, effectively creating a supervised semantic parsing dataset (e.g., Zelle & Mooney, 1996; Zettlemoyer & Collins, 2005; Suhr et al., 2018). The programs are executable in a structured representation of the environment, and allow for exact and reliable reward computation at every possible state.

Our experiments with *lilGym* show that existing models can provide non-trivial performance given sufficient training time, with multi-modal pre-training providing further benefit. However, there remains significant room for improvement. For example, on the simplest configuration, our agent can solve 76.54% of the test environments, but performance drops significantly to only 6.09% on the most complex configuration. The *lilGym* framework and trained models are available at <https://lil.nlp.cornell.edu/lilgym/>.

2 RELATED WORK

There is significant and increasing interest in RL conditioned on natural language. Various strategies are deployed to resolve language semantics for reward computation, mostly by strict control of the language or through approximations.

Maybe the most common approach is to control the language by using synthetic language backed by a formal representation (Narasimhan et al., 2015; Johnson et al., 2017a;b; Côté et al., 2018; Chevalier-Boisvert et al., 2019; Co-Reyes et al., 2019; Jiang et al., 2020). Although synthetic language allows studying the problem of learning high-level concepts, many of the complexities of natural language are stripped away, and such approaches run the risk of reducing the language learning challenge to reverse engineering the hand-crafted generation process.

An alternative that allows for natural language while retaining the control of its semantics is to generate the target sequence of decisions (i.e., task demonstration), and solicit post-hoc instructional language (Shridhar et al., 2020; 2021; Hanjie et al., 2021). While this process uses human-written language, it potentially implicitly retains the regularities of the demonstration generation procedure.

Others have carefully designed the underlying environment to simplify termination state evaluation given demonstrations, for example, with a sparse graph-based structure (Anderson et al., 2018; Chen et al., 2019; Ku et al., 2020). However, recent work shows the potential for evaluation fidelity issues even in these settings (Jain et al., 2019).

In contrast to previous approaches, we emphasize using human-written natural language and avoid constraining the task to simplify reward evaluation. We also opt to not use underlying hand-crafted procedures as stimuli for the writing. *lilGym* prioritizes exact reward computation rather than automated approximations to allow for relatively clean benchmarking of learning methods.

Our annotation of natural language statements with programs is inspired by the annotation of data for supervised learning of semantic parsers (Zelle & Mooney, 1996; Zettlemoyer & Collins, 2005; Suhr et al., 2018). The Python API of our environments is based on the semantic parsing work of Goldman et al. (2018). Robust semantic parsers can assist in automating our annotation process.

3 THE *lilGYM* BENCHMARK

lilGym consists of a collection of environments that share a common backbone. The backbone is a 2D plane that is manipulated by placing and removing objects of different types. Each environment instance is a Markov Decision Process (MDP) created by pairing a natural language statement and a target boolean value with a configuration of the shared backbone. The goal of the agent in each environment is to manipulate it by adding and removing objects so that the truth-value of the statement with regard to the environment is the target boolean.

The learning problem *lilGym* presents is to induce a policy that generalizes across MDPs. We split the MDPs to training, development, and held-out testing sets. The training environments are to be

Table 1: Data statistics per CMDP configuration and data split. The number of MDPs corresponds to the number of contexts under each CMDP. For FLIPIT, “Init.” corresponds to the total number of initial states across all MDPs for this CMDP.³

	TOWER-SCRATCH		TOWER-FLIPIT		SCATTER-SCRATCH		SCATTER-FLIPIT	
	MDPs	MDPs	Init.	MDPs	MDPs	Init.	MDPs	Init.
Train	989	1,910	5,704	1,241	2,340	6,696		
Dev	163	317	676	87	164	313		
Test	324	619	1,383	155	285	591		
Total	1,476	2,846	7,763	1,483	2,789	7,600		

used for parameter estimation, while the two other sets are for testing during development and for final held-out testing to report approach performance.²

There are two dimensions of configuration: appearance and starting condition. The appearance determines the state space, transition function, and action space. The appearance of the environment can be (a) TOWER: the objects include squares only, and they can be stacked into towers in specific positions only; or (b) SCATTER: objects of different types can be freely distributed. TOWER gives a more constrained problem with much smaller state and action spaces compared to SCATTER.

The starting condition determines the agent’s goal. The starting condition and agent’s objective can be: (a) SCRATCH: the environment starts without any objects and the goal is to modify it so that the statement’s truth-value is True; or (b) FLIPIT: the environment starts with a set of objects and the agent’s goal is to flip the truth-value of the statement. SCRATCH generally only requires adding objects, except in cases of correcting for agent’s errors, while FLIPIT requires both adding and removing, because there are already objects present.

The four configurations are TOWER-SCRATCH, TOWER-FLIPIT, SCATTER-SCRATCH, and SCATTER-FLIPIT. In our experiments (Section 5), we observe the different configurations provide different levels of difficulty. For example, SCATTER configurations are generally much harder than TOWER, as expected with the much larger state and action spaces.

Each configuration forms a Contextual Markov Decision Process (CMDP; Hallak et al., 2015). CMDP is an abstraction over a set of MDPs to account for a context that remains constant throughout an interaction with an MDP. We set the context to include the statement and the target boolean the interaction is conditioned on. A CMDP is a tuple $(\mathcal{C}, \mathcal{S}, \mathcal{A}, \mathcal{M}(c))$, where \mathcal{C} is the context space, \mathcal{S} the state space, \mathcal{A} the action space, and \mathcal{M} a function mapping a context $c \in \mathcal{C}$ to an MDP $\mathcal{M}(c) = (\mathcal{S}, \mathcal{A}, T, R^c, \beta^c)$. Here, $T : \mathcal{S} \times \mathcal{A} \rightarrow \mathcal{S}$ is a transition function, $R^c : \mathcal{S} \times \mathcal{A} \rightarrow \mathbb{R}$ a reward function, and β^c an initial state distribution. This means that a CMDP is a set of MDPs that share the same states and actions. The policy learning problem is to estimate parameters θ of a policy $\pi_\theta : \mathcal{S} \times \mathcal{C} \rightarrow \mathcal{A}$, which maps the current state and the context underlying the MDP to an action. The aim is for the policy to generalize across different contexts from \mathcal{C} . Table 1 shows the number of MDPs under each configuration. Figure 1 shows example action trajectories in MDPs for each of the four CMDPs.

Contexts \mathcal{C} A context $c \in \mathcal{C}$ is a pair $c = (\bar{x}, b)$, where \bar{x} is a natural language statement and $b \in \{\text{True}, \text{False}\}$ is a target boolean value for the statement \bar{x} with respect to the state s . The set of statements is predefined for TOWER and SCATTER based on the NLVR data, but identical across the choice of SCRATCH and FLIPIT. The target boolean value in SCRATCH is always True. In FLIPIT, the target boolean value can be either True or False. Depending on the context, different types of reasoning are required. For example, in the second column of Figure 1, the statement *there is no black block as the top of a tower with at most three blocks* requires the agent to reason about negation, soft cardinality, color, and position, while the statement in the third column

²We recommend reporting both development and held-out test results in future work for easy comparison.

³NLVR includes a total of 18,322 images. This allows further expanding the number of initial states to 92,179 initial states through box element permutations. We do not manipulate this property in this work, but future work could take advantage of it. Our reward computation is invariant to such permutations.

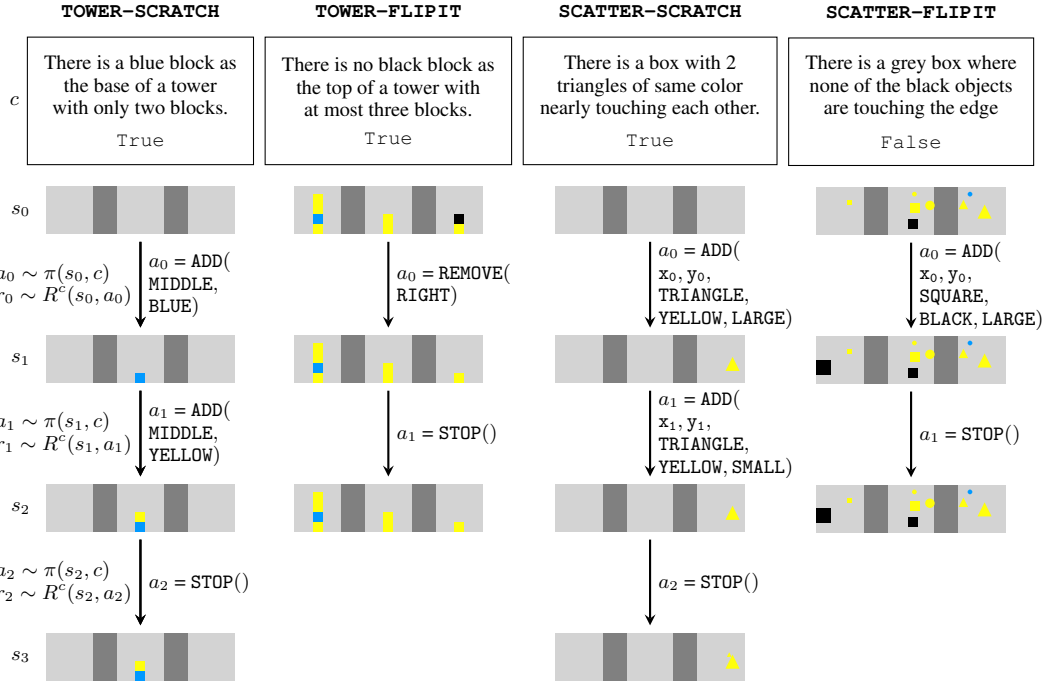


Figure 1: Examples for each of the four CMDP configurations. Each example is conditioned on a context $c = (\bar{x}, b)$, and starts with a state s_0 , sampled from the initial state distribution β^c . For example, for TOWER-SCRATCH (left column), the context c pairs the statement *there is a blue block as the base of a tower with only two blocks.* with the target boolean True. The initial state s_0 is an image with three empty light grey box regions separated by dark grey separators. The agent π is presented with (s_0, c) , and samples an action $a_0 \sim \pi(s_0, c)$. The environment transitions to the next state s_1 , while the context remains the same. This process continues until the termination condition is filled when the agent selects the STOP action.

there is a box with 2 triangles of same color nearly touching each other requires a comparison and to reason about several object attributes (shape, color, position). Both require the agent to perform high-level relational reasoning about single objects or sets.

States \mathcal{S} A state $s \in \mathcal{S}$ is an RGB image. Images in *lilGym* are divided into three box regions of identical dimensions by two dark gray separators (Figure 1). The objects in *lilGym* have three properties, each can take multiple values: shape (CIRCLE, SQUARE, or TRIANGLE), color (BLACK, BLUE, or YELLOW), and size (SMALL, MEDIUM, or LARGE). In TOWER, states are constrained to have stacks of up to four SQUARES of MEDIUM size and any color at the center of each box. SCATTER states support all object shapes, sizes, and colors, and they may be positioned freely. In both conditions, objects cannot cross image boundaries or into the separators. The choice of starting condition between SCRATCH or FLIPIT does not influence the state space.

Actions \mathcal{A} and Transitions \mathcal{T} There are three action types STOP, ADD, and REMOVE. STOP terminates the episode and does not require any parameters. The truth-value of the statement is only evaluated and compared to the target boolean after the STOP action is taken. ADD adds objects to the environment, and REMOVE removes objects.

Both ADD and REMOVE take arguments that differ between TOWER and SCATTER:

TOWER: Similar to the state space of TOWER, the actions are also constrained. Both ADD and REMOVE take a position argument, which has three possible values corresponding to the three box regions. Objects are always added or removed at the top of the stack. Adding an object on top of a stack of four objects or removing an object from an empty box are both invalid actions. ADD also takes a color argument. For example, the first action on

the left trajectory in Figure 1 is adding a blue square in an empty box. Including STOP, there are $1 + (3 + 1) \times 3 = 13$ actions.

SCATTER: Unlike TOWER, objects of any type can be placed freely in the box regions. Both ADD and REMOVE take 2D coordinates that specify the pixel location. Adding an object places it so that its top-left coordinates are the given coordinates. Removing an object will remove the object at the given coordinates. Adding also requires specifying the shape, color, and size. The action is invalid if adding results in objects’ overlap or boundary crossing with the separators or image boundaries. Removing from a position that does not include an object is also an invalid action. The native resolution of images in *lilGym* is 380×100 pixels. Including STOP, there are $1 + (380 \times 100) \times ((3 \times 3 \times 3) + 1) = 1,064,001$ actions. Because of the extremely large action space, *lilGym* also supports a simplification through a coarser grid system for SCATTER that is automatically mapped to the original resolution (Appendix A). The grid simplification includes heuristics that assist in identifying locations to place objects in the original pixel space or objects to remove once a grid cell is selected. Without these heuristics, a grid system that is coarser than the original resolution would result in a large number of MDPs become unsolvable (e.g., when a statement requires objects to touch). In our experiments (Section 5), we use a grid simplification of 19×5 , giving a total of 2,661 actions. The difficulty of SCATTER can be adjusted by modifying the grid size, or acting at the original resolution.

The transition function $T : \mathcal{S} \times \mathcal{A} \rightarrow \mathcal{S}$ depends on the choice between TOWER and SCATTER configurations, because this choice determines the action space. Similar to the action space, the transitions in TOWER are more constrained compared to SCATTER. The transition function does not modify the context, which is fixed for a given MDP.

Reward Function R^c The reward function R^c is computed with respect to the context pair $c = (\bar{x}, b)$, and is based on evaluating the truth-value of the natural language statement \bar{x} with respect to a state s , and comparing it to the target boolean b . *lilGym* includes an executable evaluation function $\mathcal{E}^{\bar{x}} : \mathcal{S} \times \mathcal{A} \rightarrow \{\text{True}, \text{False}\}$ for every statement \bar{x} . Section 4 describes how we create the evaluation functions.

The agent receives a positive reward for terminating the episode using the STOP action with the statement evaluation $\mathcal{E}^{\bar{x}}(s)$ equal to the target boolean value b . If the statement boolean value $\mathcal{E}^{\bar{x}}(s)$ does not equal the target boolean b value when taking the STOP action, the agent receives a negative reward. If the episode terminates because the current time step t reached the action horizon H or because of an invalid action, the agent also receives a negative reward. Action validity depends on the current state s and on the configuration, because TOWER and SCATTER have different action spaces. For example, in TOWER, adding an object to a box (e.g., ADD(MIDDLE, BLUE)) is only valid if the box has less than four objects, because towers have a maximum height of four. There is also a verbosity penalty of δ for every other action. Formally, the reward is:

$$R^c(s, a) = \begin{cases} 1.0 & a = \text{STOP} \wedge \mathcal{E}^{\bar{x}}(s) = b \\ -1.0 & a = \text{STOP} \wedge \mathcal{E}^{\bar{x}}(s) \neq b \\ -1.0 & (a \text{ is invalid in } s) \vee (t = H) \\ -\delta & \text{otherwise} \end{cases}.$$

Initial State Distribution β^c The initial state distribution β^c is parameterized by the context $c \in \mathcal{C}$, which is different between SCRATCH and FLIPIT. In SCRATCH, the agent modifies an empty environment to satisfy the truth-condition of the statement \bar{x} in the context c , so the initial state s_0 is always an empty image. The set of initial states β^c for every context $c \in \mathcal{C}$ is the set of images associated with the statement \bar{x} in the NLVR data. In practice, for FLIPIT, this set includes between 1 to 43 images. Table 1 shows the total number of initial states in each configuration.

4 THE *lilGYM* DATA

The data used for *lilGym* is based on the NLVR corpus (Suhr et al., 2017). The NLVR data was initially collected as a supervised learning benchmark. We formalize an interactive task on top of the NLVR data and collect additional annotations for reward computation.

4.1 BACKGROUND: THE NLVR CORPUS

NLVR includes human-written natural language statements paired with synthetic images. Each pair is annotated with the boolean truth-value of the statement with regard to the image (i.e., `True` if the statement is true with regard to the image, or `False` otherwise). The images are designed to support complex reasoning, including about spatial and set relations. The original learning task posed by NLVR is to classify statement-image pairs as `True` to indicate the statement is true with regard to the image, or `False` otherwise. Various approaches were developed to address the NLVR challenge (Suhr et al., 2017; Tan & Bansal, 2018; Goldman et al., 2018; Pavez et al., 2018; Yao et al., 2018; Hudson & Manning, 2018; Perez et al., 2018; Dasigi et al.; Zheng et al., 2020; Gupta et al., 2021), and a separate version using photos was also released (Suhr et al., 2019).⁴

Qualitative analysis of the data (Table 2 in Suhr et al., 2017) shows a more diverse representation of semantic and compositional phenomena compared to related corpora (Antol et al., 2015), including requiring joint visual-linguistic reasoning about spatial relations, quantities, and sets of objects. NLVR also provides an underlying structured representation for every image, which supports easy image manipulation. The combination of a simple interface for image manipulation with complex reasoning via natural language makes NLVR ideal to support an interactive benchmark environment.

4.2 CONSTRUCTING *li*GYM FROM NLVR

We use the NLVR data to create each of the CMDPs (Table 1). SCRATCH CMDPs include contexts for all natural language statements from NLVR, each paired with the empty initial state containing no shapes (Figure 1, left and center right columns). FLIPIT CMDPs include the natural language statements with their corresponding images, both from NLVR. The images are used as initial states. The target boolean is set so that the initial state does not fulfil it. The split between TOWER and SCATTER also follows from NLVR. Statements corresponding to TOWER images in NLVR are included in our TOWER CMDPs, and the same for SCATTER sentences.

NLVR has four splits for training, development, public testing, and hidden testing. We follow the original splits for the training and development sets. Following the recent public release of the hidden testing set, we merge the public and hidden testing sets into a single public test split.

4.3 ANNOTATIONS FOR REWARD COMPUTATION

The NLVR annotations include the truth-value of each statement with regard to the images paired with it in the data. Once we manipulate an image (i.e., change the state in our interactive environment), the truth-value annotation does not hold. A key challenge for creating an interactive environment using the NLVR data is the need for an accurate evaluation of the natural language statement for *every* possible state (i.e., image), as required for reward computation (Section 3).

We address this challenge by annotating each statement \bar{x} with an executable boolean Python program representing its meaning, $\mathcal{E}^{\bar{x}}$ in Section 3. The Python programs operate on the underlying structured representation. Each program returns `True` for every image that satisfies the constraints specified in the corresponding statement, and `False` otherwise. In general, there are many states that satisfy any given statement, many more than provided with the original NLVR images.

The programs are written using an API defined over the structured representations. We base the API design on the logical ontology designed for NLVR’s structured representations by Goldman et al. (2018), which we extend to include a total of 66 functions. Figure 4 in Appendix B shows two examples of logical forms paired with their corresponding statements.

We use the freelancing platform Upwork⁵ for annotation. We recruit three annotators based on preliminary screening of their fluency in English and competency in Python. We de-duplicate the naturally occurring sentences in the data, collect 2,666 annotations at a total cost of \$3,756, and keep 2,661 valid annotations.

All the sentences in the dataset are randomly distributed to the annotators, each with an example image. Every sentence is annotated with a logical form by one annotator. Each logical form is

⁴We do not use the photographic NLVR2 in this work.

⁵<https://www.upwork.com>

evaluated against a corresponding hidden validation set, and must pass all the tests. Appendix B describes our annotation and validation process.

5 EXPERIMENTS

5.1 METHODS

We experiment with each of the four CMDPs separately, training on the training data and testing on the development and held-out test splits. We sample a validation set from the training data for model selection. For SCATTER we use the simplified grid action space with a grid of 19×5 (Section 3). Each grid cell is of size 20×20 pixels. We set the action horizon $H = 12$. Appendix C provides more details about our setup.

We use PPO (Schulman et al., 2017) for parameter estimation,⁶ with a separate network as a critic. The critic network is identical to the policy, except that we add a tanh activation for the value output. Because of the large action space, especially for SCATTER, the agent rarely observes positive reward, which requires taking a STOP action at an appropriate state. We design a simple variant of PPO called PPO+SF (PPO with stop forcing) to study this issue. PPO+SF is identical to PPO, except that during training, we mask all actions except STOP when the agent reaches a state where selecting STOP will give a positive reward. This modification is present only during training. All testing is done under the same conditions, without stop forcing.

We experiment with two models:

C+BERT We process the statement \bar{x} using BERT (Devlin et al., 2019), and do mean pooling across all layers and tokens to get the statement representation. We use a three-layer CNN (Fukushima & Miyake, 1982) to embed the image of the current state s . We concatenate the statement representation, image representation, and an embedding for the target boolean b , and process the vector through a multi-layer perceptron (MLP) to compute the action distribution.

ViLT ViLT is a pretrained multi-modal Transformer that jointly processes text and image inputs (Kim et al., 2021). We create a sequence of tokens by concatenating the statement, a token for the target boolean, and image patches, separated by special tokens. The image patches are the same size as the 19×5 grid cells, including in TOWER, where the action space does not use a grid.

5.2 RESULTS AND ANALYSIS

Table 2 shows development and test set accuracies for all CMDPs. Figure 2 breaks down development set accuracies for FLIPIT CMDPs by the target boolean, and Figure 3 shows development rollout statistics. We also sample 50 development examples for each CMDP, and annotate them with expert⁷ trajectories to estimate the expert reward and rollout statistics.

The additional guidance of PPO+SF compared to PPO helps with exploration, especially on SCATTER CMDPs (Table 2). On SCATTER-FLIPIT, PPO+SF improves performance by 23.86% compared to PPO. This illustrates the hard exploration problem that SCATTER CMDPs pose.

ViLT generally outperforms C+BERT, except on SCATTER-SCRATCH (Table 2). This is relatively expected given the joint reasoning architecture and multi-modal pre-training of ViLT. FLIPIT policies generally do better on examples with a `False` target boolean, except when learning fails (Figure 2). The other direction is harder, because the set of states that invalidates a statement is usually larger than the set that validates it, and it generally requires fewer actions to invalidate a statement.

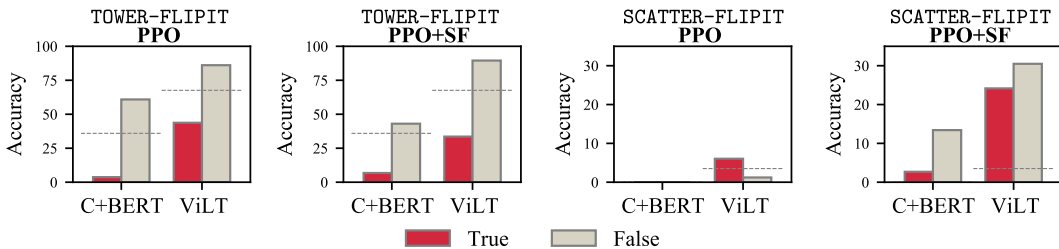
We observe more rollouts that are terminated by reaching the action horizon H (i.e., without STOP) on TOWER CMDPs compared to SCATTER (Figure 3, left). This difference is partially explained by a higher rate of invalid actions in SCATTER (Figure 3, center left), which cause immediate rollout termination. In general, ViLT has a higher rate of invalid actions, except on SCATTER-FLIPIT with PPO, where overall performance is extremely low. We also see more non-stopped rollouts for

⁶We use the PPO implementation of Kostrikov (2018).

⁷The expert is an author of this paper.

Table 2: Accuracies for all the four CMDP. Evaluation is always without stop forcing.

		TOWER-SCRATCH		TOWER-FLIPIT		SCATTER-SCRATCH		SCATTER-FLIPIT	
		Dev	Test	Dev	Test	Dev	Test	Dev	Test
PPO	C+BERT	71.78	63.27	35.95	34.78	39.08	48.39	0.00	0.00
	ViLT	81.60	76.54	67.60	65.80	35.63	41.29	3.51	6.09
PPO+SF	C+BERT	80.98	78.70	27.22	26.75	70.12	74.84	8.31	8.46
	ViLT	84.05	82.41	65.09	62.91	64.37	70.97	27.48	29.95

Figure 2: Development set accuracies for FLIPIT CMDPs, reported according to the value of the context target boolean. **Red**: target is True. **Gray**: target is False. **Dashed gray line**: accuracy on the full development set.

TOWER-FLIPIT when training with PPO+SF. These rollouts often correspond to the model getting stuck in add-remove loops.

There is no consistent difference in the length of rollouts between the two models (Figure 3, center right). Model trajectory length is similar on TOWER, where models perform fairly well. However, on SCATTER, where our models are weaker, human trajectories are significantly longer. This is partially explained by the model not learning to effectively avoid invalid actions, which terminate the execution immediately. In general, we observe no significant effective learning of using REMOVE actions. TOWER-FLIPIT is an exception with REMOVE dominating the rollouts (Figure 3, right), potentially because removing objects generally provides a more efficient path to flip the boolean value. While PPO policies generate REMOVE actions for SCATTER-FLIPIT, the extremely low performance indicates that these actions are not used effectively. Human statistics indicate that REMOVE actions are beneficial for FLIPIT CMDPs. Even though some of these examples can be solved with ADD actions only, removing objects often provides a more efficient path. While TOWER-FLIPIT models leverage this, SCATTER-FLIPIT models do not. This is potentially because REMOVE actions require positional precision that is harder to acquire in SCATTER.

We compute the mean reward for each model for development examples, and compare them to the expert reward estimate (Table 3). ViLT always performs better than C+BERT. There is significant room to improve model performance and efficiency. For example, on TOWER-FLIPIT, the estimated expert mean reward is 0.83, while ViLT trained with PPO, the best of our models, gets a reward of 0.22.

Suhr et al. (2017) manually annotated 200 development examples for semantic phenomena. Table 4 shows the performance on this data of policies trained with PPO. We only include categories with more than 10 instances across all CMDPs. Appendix D.3 provides the complete tables with examples, including for PPO+SF. The two models mostly follow similar trends with respect to the categories on which they perform above and below overall performance. A notable exception is coordination, where ViLT performs above overall performance on 2/4 CMDPs, while C+BERT always performs below. We also observe a difference between TOWER and SCATTER on soft cardinality (e.g., *... at least two ...*), with above average performance on TOWER and below on SCATTER.

Appendix D includes further analysis. Most errors are due to invalid actions (Appendix D.1), and that models are biased towards focusing on specific positions and other action arguments (Appendix D.2), even if these lead to invalid actions and rollout failure.

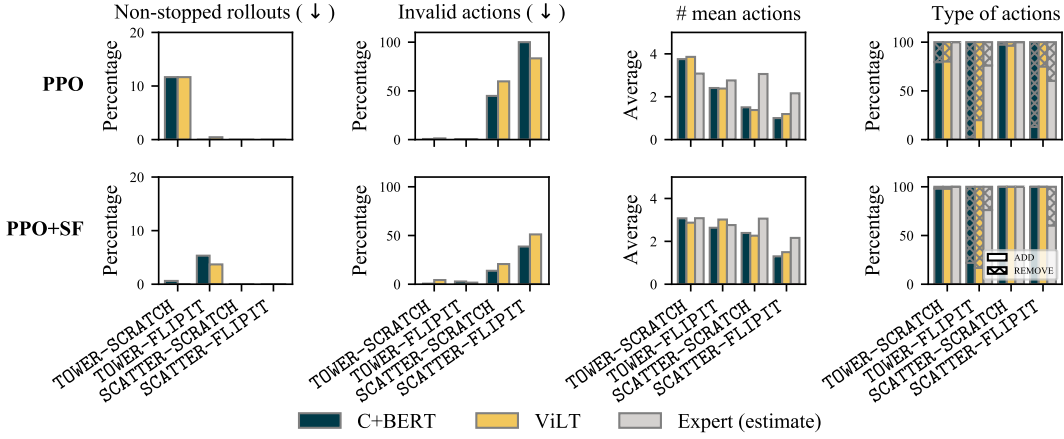


Figure 3: Development rollout statistics, from left to right: percentage of rollouts that reach the action horizon without a STOP action; percentage of rollouts with an invalid action; mean actions per rollout; percentage of ADD/REMOVE actions. Expert statistics are estimated from 50 randomly sampled human-annotated examples. ↓ shows the preferred direction.

Table 3: Mean development set rewards. Expert reward are estimated on 50 examples. All human rollouts are successful.

		TOWER-SCRATCH	TOWER-FLIPIT	SCATTER-SCRATCH	SCATTER-FLIPIT
Expert		0.79	0.83	0.79	0.89
PPO	C+BERT	0.27	-0.42	-0.27	-1.00
	ViLT	0.45	0.22	-0.33	-0.95
PPO+SF	C+BERT	0.42	-0.57	0.26	-0.86
	ViLT	0.49	0.13	0.16	-0.50

6 CONCLUSION

We introduce *lilGym*, a reinforcement learning benchmark that focuses on natural language visual reasoning. *lilGym* is designed to be accessible for RL researchers, while still displaying the reasoning richness of natural language. It is relatively easy to deploy using the standard OpenAI Gym API (Brockman et al., 2016), and has light compute requirements. Our data annotation approach allows including expressive and diverse natural language, while still providing accurate and automatic reward computation. This allows *lilGym* to balance between posing a challenging research problem and avoiding engineering challenges or approximation costs. Our strong baselines illustrate the range of challenges *lilGym* presents, showing that existing methods can achieve non-trivial performance, but that there remain significant challenges to be solved and progress to be made. Our analysis lays out the framework for studying and reporting these future results.

lilGym also has significant potential beyond the tasks we study. It can be used without the language, to create thousands of micro RL tasks requiring set and relational visual reasoning. Our annotations form a new semantic parsing corpus with annotated executable meaning representations. The semantic diversity of the data, its executability, and the focus on visual reasoning make it a unique asset in the landscape of corpora for semantic parsing. *lilGym* is also promising for program synthesis, where the combination of language and example data fits recent focus on guiding synthesis using language (Wong et al., 2021).

Table 4: Performance on a set of development examples annotated for semantic categories by Suhr et al. (2017) for both models (C+BERT | ViLT) when trained with PPO. Dev performance refers to mean performance on the respective full development set. Results outperforming dev performance are in bold.

	TOWER-SCRATCH			TOWER-FLIPIT			SCATTER-SCRATCH			SCATTER-FLIPIT		
	Total	Correct %		Total	Correct %		Total	Correct %		Total	Correct %	
Cardinality (hard)	98	67.3	78.6	480	36.7	70.8	35	31.4	37.1	119	0.0	5.0
Cardinality (soft)	21	81.0	85.7	82	43.9	65.9	11	9.1	18.2	42	0.0	2.4
Existential	122	73.8	83.6	577	37.6	70.7	55	36.4	32.7	192	0.0	3.6
Coordination	19	31.6	52.6	86	29.1	70.9	15	20.0	40.0	55	0.0	0.0
Spatial Relations	93	77.4	87.1	438	39.7	69.2	39	41.0	30.8	128	0.0	5.5
Presupposition	17	47.1	58.8	74	35.1	68.9	22	40.9	40.9	78	0.0	5.1
Dev performance		71.78	81.60		35.95	67.60		39.08	35.63		0.00	3.51

ACKNOWLEDGEMENTS

This research was supported by ARO W911NF21-1-0106, NSF under grant No. 1750499, a gift from Open Philanthropy, and NSF under grant No. 2127309 to the Computing Research Association for the CIFellows Project. Results presented in this paper were obtained using CloudBank (Norman et al., 2021), which is supported by the National Science Foundation under award No. 1925001. We thank Alane Suhr, Ge Gao, Justin Chiu, Woojeong Kim, Jack Morris, Jacob Sharf and the Cornell NLP Group for support, comments and helpful discussions.

REFERENCES

Peter Anderson, Qi Wu, Damien Teney, Jake Bruce, Mark Johnson, Niko Sünderhauf, Ian Reid, Stephen Gould, and Anton van den Hengel. Vision-and-language navigation: Interpreting visually-grounded navigation instructions in real environments. In *The IEEE Conference on Computer Vision and Pattern Recognition*, pp. 3674–3683, 2018.

Stanislaw Antol, Aishwarya Agrawal, Jiasen Lu, Margaret Mitchell, Dhruv Batra, C. Lawrence Zitnick, and Devi Parikh. VQA: Visual question answering. In *IEEE International Conference on Computer Vision*, pp. 2425–2433, 2015.

Greg Brockman, Vicki Cheung, Ludwig Pettersson, Jonas Schneider, John Schulman, Jie Tang, and Wojciech Zaremba. Openai gym, 2016.

Howard Chen, Alane Suhr, Dipendra Misra, Noah Snavely, and Yoav Artzi. Touchdown: Natural language navigation and spatial reasoning in visual street environments. In *Proceedings of the IEEE/CVF Conference on Computer Vision and Pattern Recognition*, pp. 12538–12547, 2019.

Maxime Chevalier-Boisvert, Dzmitry Bahdanau, Salem Lahlou, Lucas Willems, Chitwan Saharia, Thien Huu Nguyen, and Yoshua Bengio. Babyai: A platform to study the sample efficiency of grounded language learning. In *7th International Conference on Learning Representations, ICLR*, 2019.

John D. Co-Reyes, Abhishek Gupta, Suvansh Sanjeev, Nick Altieri, John DeNero, P. Abbeel, and Sergey Levine. Guiding policies with language via meta-learning. In *7th International Conference on Learning Representations, ICLR*, 2019.

Marc-Alexandre Côté, Ákos Kádár, Xingdi Yuan, Ben A. Kybartas, Tavian Barnes, Emery Fine, James Moore, Matthew J. Hausknecht, Layla El Asri, Mahmoud Adada, Wendy Tay, and Adam Trischler. Textworld: A learning environment for text-based games. In *CGW@IJCAI*, 2018.

Pradeep Dasigi, Matt Gardner, Shikhar Murty, Luke Zettlemoyer, and Eduard Hovy. Iterative search for weakly supervised semantic parsing. In *Proceedings of the 2019 Conference of the North*

American Chapter of the Association for Computational Linguistics: Human Language Technologies, Volume 1 (Long and Short Papers), pp. 2669–2680.

Jacob Devlin, Ming-Wei Chang, Kenton Lee, and Kristina Toutanova. BERT: Pre-training of deep bidirectional transformers for language understanding. In *Proceedings of the 2019 Conference of the North American Chapter of the Association for Computational Linguistics: Human Language Technologies, Volume 1 (Long and Short Papers)*, pp. 4171–4186, 2019.

Kunihiro Fukushima and Sei Miyake. Neocognitron: A self-organizing neural network model for a mechanism of visual pattern recognition. In *Competition and cooperation in neural nets*, pp. 267–285. Springer, 1982.

Omer Goldman, Veronica Latchinnik, Ehud Nave, Amir Globerson, and Jonathan Berant. Weakly supervised semantic parsing with abstract examples. In *Proceedings of the 56th Annual Meeting of the Association for Computational Linguistics (Volume 1: Long Papers)*, pp. 1809–1819, 2018.

Nitish Gupta, Sameer Singh, and Matt Gardner. Enforcing consistency in weakly supervised semantic parsing. In *Proceedings of the 59th Annual Meeting of the Association for Computational Linguistics and the 11th International Joint Conference on Natural Language Processing (Volume 2: Short Papers)*, pp. 168–174, 2021.

Assaf Hallak, Dotan Di Castro, and Shie Mannor. Contextual markov decision processes. *arXiv preprint arXiv:1502.02259*, 2015.

Austin W Hanjie, Victor Y Zhong, and Karthik Narasimhan. Grounding language to entities and dynamics for generalization in reinforcement learning. In *International Conference on Machine Learning*, pp. 4051–4062. PMLR, 2021.

Drew A. Hudson and Christopher D. Manning. Compositional attention networks for machine reasoning. In *6th International Conference on Learning Representations, ICLR*, 2018.

Vihan Jain, Gabriel Magalhaes, Alexander Ku, Ashish Vaswani, Eugene Ie, and Jason Baldridge. Stay on the path: Instruction fidelity in vision-and-language navigation. In *Proceedings of the Annual Meeting of the Association for Computational Linguistics*, pp. 1862–1872, July 2019.

Minqi Jiang, Jelena Luketina, Nantas Nardelli, Pasquale Minervini, Philip HS Torr, Shimon Whiteson, and Tim Rocktäschel. Wordcraft: An environment for benchmarking commonsense agents. *arXiv preprint arXiv:2007.09185*, 2020.

Justin Johnson, Bharath Hariharan, Laurens Van Der Maaten, Li Fei-Fei, C Lawrence Zitnick, and Ross Girshick. Clevr: A diagnostic dataset for compositional language and elementary visual reasoning. In *Proceedings of the IEEE conference on computer vision and pattern recognition*, pp. 2901–2910, 2017a.

Justin Johnson, Bharath Hariharan, Laurens van der Maaten, Judy Hoffman, Li Fei-Fei, C. Lawrence Zitnick, and Ross B. Girshick. Inferring and executing programs for visual reasoning. *2017 IEEE International Conference on Computer Vision (ICCV)*, pp. 3008–3017, 2017b.

Wonjae Kim, Bokyung Son, and Ildoo Kim. Vilt: Vision-and-language transformer without convolution or region supervision. In *Proceedings of the 38th International Conference on Machine Learning*, pp. 5583–5594, 2021.

Diederik P. Kingma and Jimmy Ba. Adam: A method for stochastic optimization. In Yoshua Bengio and Yann LeCun (eds.), *3rd International Conference on Learning Representations, ICLR*, 2015.

Ilya Kostrikov. Pytorch implementations of reinforcement learning algorithms, 2018.

Alexander Ku, Peter Anderson, Roma Patel, Eugene Ie, and Jason Baldridge. Room-across-room: Multilingual vision-and-language navigation with dense spatiotemporal grounding. In *Proceedings of the 2020 Conference on Empirical Methods in Natural Language Processing (EMNLP)*, pp. 4392–4412, 2020.

Ilya Loshchilov and Frank Hutter. Decoupled weight decay regularization. In *7th International Conference on Learning Representations, ICLR*, 2019.

Dipendra Kumar Misra, John Langford, and Yoav Artzi. Mapping instructions and visual observations to actions with reinforcement learning. In *Proceedings of the 2017 Conference on Empirical Methods in Natural Language Processing, EMNLP7*, pp. 1004–1015, 2017.

Karthik Narasimhan, Tejas D. Kulkarni, and Regina Barzilay. Language understanding for text-based games using deep reinforcement learning. In *Proceedings of the 2015 Conference on Empirical Methods in Natural Language Processing, EMNLP*, pp. 1–11, 2015.

Michael Norman, Vince Kellen, Shava Smallen, Brian DeMeulle, Shawn Strande, Ed Lazowska, Naomi Alterman, Rob Fatland, Sarah Stone, Amanda Tan, Katherine Yelick, Eric Van Dusen, and James Mitchell. Cloudbank: Managed services to simplify cloud access for computer science research and education. In *Practice and Experience in Advanced Research Computing, PEARC '21*. Association for Computing Machinery, 2021.

Juan Pavez, Héctor Allende, and Héctor Allende-Cid. Working memory networks: Augmenting memory networks with a relational reasoning module. In *Proceedings of the 56th Annual Meeting of the Association for Computational Linguistics (Volume 1: Long Papers)*, pp. 1000–1009, 2018.

Ethan Perez, Florian Strub, Harm De Vries, Vincent Dumoulin, and Aaron Courville. Film: Visual reasoning with a general conditioning layer. In *Proceedings of the AAAI Conference on Artificial Intelligence*, volume 32, 2018.

John Schulman, Filip Wolski, Prafulla Dhariwal, Alec Radford, and Oleg Klimov. Proximal policy optimization algorithms. *arXiv preprint arXiv:1707.06347*, 2017.

Mohit Shridhar, Jesse Thomason, Daniel Gordon, Yonatan Bisk, Winson Han, Roozbeh Mottaghi, Luke Zettlemoyer, and Dieter Fox. ALFRED: A benchmark for interpreting grounded instructions for everyday tasks. In *2020 IEEE/CVF Conference on Computer Vision and Pattern Recognition, CVPR*, 2020.

Mohit Shridhar, Xingdi Yuan, Marc-Alexandre Côté, Yonatan Bisk, Adam Trischler, and Matthew J. Hausknecht. Alfworld: Aligning text and embodied environments for interactive learning. In *9th International Conference on Learning Representations, ICLR*, 2021.

Alane Suhr, Mike Lewis, James Yeh, and Yoav Artzi. A corpus of natural language for visual reasoning. In *Proceedings of the 55th Annual Meeting of the Association for Computational Linguistics (Volume 2: Short Papers)*, pp. 217–223, 2017.

Alane Suhr, Srinivasan Iyer, and Yoav Artzi. Learning to map context-dependent sentences to executable formal queries. In *Proceedings of the Conference of the North American Chapter of the Association for Computational Linguistics: Human Language Technologies*, pp. 2238–2249, 2018.

Alane Suhr, Stephanie Zhou, Ally Zhang, Iris Zhang, Huajun Bai, and Yoav Artzi. A corpus for reasoning about natural language grounded in photographs. In *Proceedings of the 57th Annual Meeting of the Association for Computational Linguistics*, pp. 6418–6428, 2019.

Hao Tan and Mohit Bansal. Object ordering with bidirectional matchings for visual reasoning. In *Proceedings of the 2018 Conference of the North American Chapter of the Association for Computational Linguistics: Human Language Technologies, Volume 2 (Short Papers)*, pp. 444–451, 2018.

Catherine Wong, Kevin Ellis, Joshua B. Tenenbaum, and Jacob Andreas. Leveraging language to learn program abstractions and search heuristics. In *Proceedings of the 38th International Conference on Machine Learning, ICML*, pp. 11193–11204, 2021.

Yiqun Yao, Jiaming Xu, Feng Wang, and Bo Xu. Cascaded mutual modulation for visual reasoning. In *Proceedings of the 2018 Conference on Empirical Methods in Natural Language Processing*, pp. 975–980, 2018.

J.M. Zelle and Raymond J. Mooney. Learning to parse database queries using inductive logic programming. In *Proceedings of the National Conference on Artificial Intelligence*, 1996.

Luke S. Zettlemoyer and Michael Collins. Learning to map sentences to logical form: Structured classification with probabilistic categorial grammars. In *Proceedings of the Conference on Uncertainty in Artificial Intelligence*, 2005.

Wenbo Zheng, Lan Yan, Chao Gou, and Fei-Yue Wang. Webly supervised knowledge embedding model for visual reasoning. *2020 IEEE/CVF Conference on Computer Vision and Pattern Recognition (CVPR)*, pp. 12442–12451, 2020.

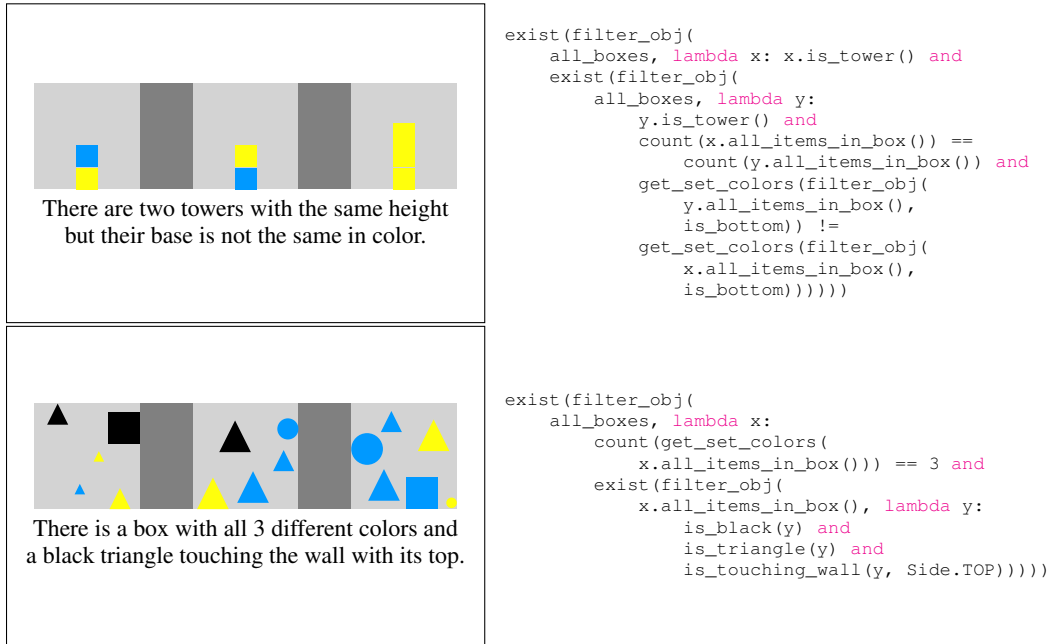


Figure 4: Example sentences with the example images displayed alongside them during annotation (left), and their annotated Python program representation (right). Both sentences and logical forms are True for the corresponding image.

A SCATTER GRID SIMPLIFICATION

To reduce the large action space of SCATTER, *litGym* allows to simplify the pixel-based action space with a grid that is coarser than the image resolution of 380×100 . The actions applied in the environment remain in the original resolution, and the translation between the grid system to pixels is done heuristically. Without the heuristics, the transition to a grid coarser than the original image resolution would render many of the MPDs unsolvable.

The heuristics simplify two translation problems: in what pixel exactly to place an object and which object to remove from a grid cell. Depending on the grid size, it is possible to add multiple objects in a cell. To find the exact pixel within a cell to add an object, we search for a pixel in the grid box where we can add the object starting from the upper left corner. We can add an object in a pixel if the object fits there without overlapping with other objects, the image boundaries, or the columns. We also snap objects to touch each other if the distance between them is below a threshold. This is to allow adding objects that *touch* each other, a common constraint in *litGym* statements. When removing an object from a grid cell, we remove the object with largest overlap with the cell.

B NATURAL LANGUAGE ANNOTATION DETAILS

We annotate each natural language statement in the NLVR corpus with a Python program representing its meaning. The programs return a boolean value, and are executable given the structured representation underlying each image. Figure 4 shows two examples of text statements with their annotate programs.

We provide the annotators with a web-based annotation interface (Figure 5), a tutorial, and an application programming interface (API) presenting a set of functions, classes and objects that they can use for annotation. We ask the annotators to prioritize the faithfulness of the program to the natural language sentence and to prefer shorter annotations. We also provide them with examples of spurious logical forms and ask them to avoid such expressions. Annotators can raise questions in case of doubts.

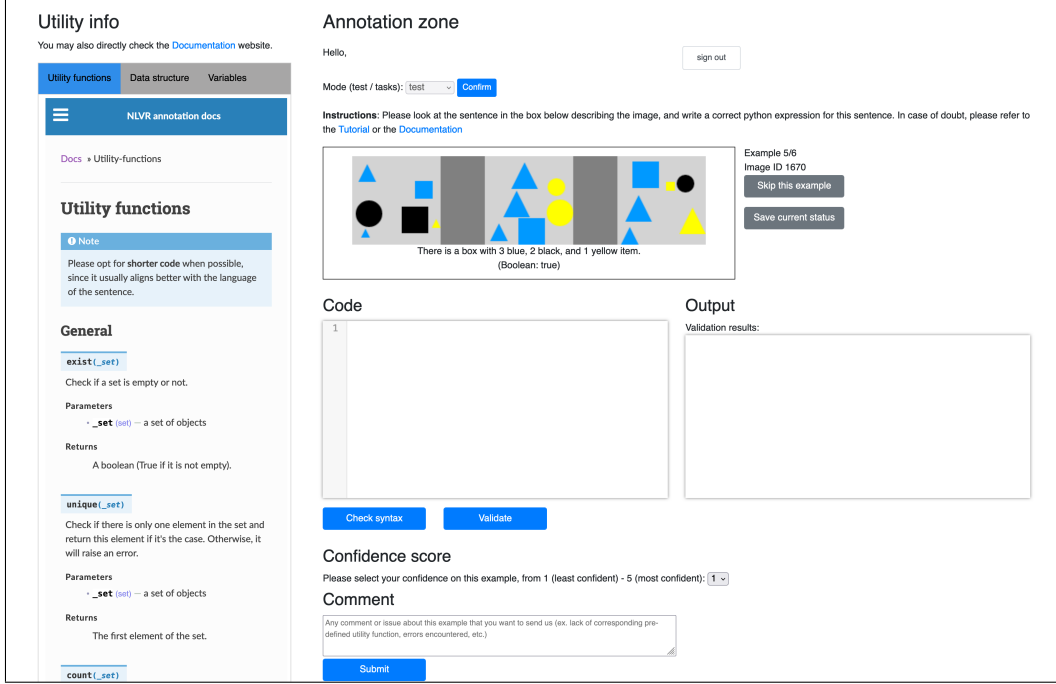


Figure 5: The annotation interface for collecting the Python program annotations in *lilGym*.

Figure 5 shows the annotation interface for a single sentence. For every sentence, annotators are provided with a single example image from NLVR and an associated boolean value. Other images for the same statement from NLVR are used as hidden validation images. The annotator never sees these images.

The annotator can validate the program syntax and validate it within the browser. The validation executes the program against the given image and all hidden images. Validation passes only once the program returns the expected boolean value for all examples, including the visible and the hidden ones. The annotator can only submit their annotation after passing the syntax check and validation. They can assign a confidence score to their annotation and provide a comment.

Annotators can skip examples in case of doubt. When skipping, they need to explicitly provide the reason. We assess the annotations by batch, then randomly redistribute the skipped examples or examples with problematic annotations to the annotators after the questions have been solved. We iteratively communicate with the workers throughout the entire annotation process.

C EXPERIMENTAL SETUP DETAILS

C.1 LEARNING DETAILS

Hyperparameters For C+BERT, we optimize using Adam (Kingma & Ba, 2015) with a learning rate of 3e-4, except on TOWER-FLIPIT trained with PPO+SF and on SCATTER-FLIPIT, where we use 3e-5. For ViLT, we use AdamW (Loshchilov & Hutter, 2019) with a cosine scheduler and a base learning rate of 3e-5 for all experiments, except on SCATTER-SCRATCH trained with PPO+SF where we use 3e-4. The learning rate is warmed up for 1% of the maximal total training steps of 4M. We use patience for early stopping. We set entropy to 0.3 for all our experiments. We use a mini-batch of 64 actions for gradient updates. At each PPO iteration we sample 2,048 actions (i.e., for the internal update loop).

PPO+SF Details PPO+SF is a simple variant of PPO that applies masking to all the actions except for STOP when the agent reaches a state in which it will receive a positive reward if it selects STOP. Via this mechanism PPO+SF allows the learner to observe STOP with positive reward with better

probability than random. A side effect of this masking is that the learner often samples action with very low probability, which can lead to exploding gradients. We clip the PPO ratio to address this. Formally, the original PPO objective is:

$$L(\theta) = \mathbb{E}_t \left[\min(r_t(\theta) \hat{A}_t, \text{clip}(r_t(\theta), 1 - \epsilon, 1 + \epsilon) \hat{A}_t) \right], \quad (1)$$

where $r_t(\theta) = \frac{\pi_\theta(a_t|s_t)}{\pi_{old}(a_t|s_t)}$, \hat{A} is the advantage function, and ϵ is a hyperparameter (Schulman et al., 2017). In PPO+SF, we clip the ratio term $r_t(\theta)$ to avoid very large value due to “force” sampling of actions with very low probability:

$$\hat{r}_t(\theta) = \min(r_t(\theta), M), \quad (2)$$

where M is a threshold bounding the ratio. We use $\hat{r}_t(\theta)$ in place of $r_t(\theta)$ for our experiments.

C.2 INFERENCE DETAILS

There are three action types STOP, ADD, and REMOVE. Each type take a different number of arguments: STOP takes not arguments, ADD takes two arguments in TOWER and five in SCATTER, and REMOVE takes one argument in TOWER and two in SCATTER. During inference, actions a are sampled from the agent policy $a \sim \pi(\cdot|s, c)$, where s is a state and c is a context. We decompose the probability of an action to be a product of its type and arguments. This risks assigning generally lower probability to actions with more arguments, because of the multiplicative decomposition. We avoid this by sampling the required arguments as needed. We first sample an action type. Depending on the action type, we sample the required arguments. In practice, this means that when an argument slot is not used the probability of that action marginalizes over all possible assignments to that argument slot.

D ADDITIONAL RESULTS AND ANALYSIS

D.1 ERROR ANALYSIS

We diagnose model errors by sampling 50 erroneous development examples for each of the two SCATTER CMDPs trained with PPO:

SCATTER-SCRATCH with C+BERT: 76% of the errors are due to invalid actions, and 24% due to early termination. Among the invalid actions, 58% are due to trying to put an item that cannot fit in the box, 24% are due to trying to perform an action on a separator, and 18% due to trying to remove an object from a position that does not include an object.

SCATTER-SCRATCH with ViLT: all errors are due to invalid actions. Among the invalid actions, 90% are due to trying to perform an action on a separator, and 10% due to trying to remove an object from a position that does not include an object.

SCATTER-FLIPIT with C+BERT: all errors are due to invalid actions. Among the invalid actions, 84% are due to trying to remove an object from a position that does not include an object, 8% are due to trying to perform an action on a separator, 4% are due to trying to put an item that cannot fit in the box, and 4% are due to trying to add an object on top of an existing one.

SCATTER-FLIPIT with ViLT: 90% of the mistakes are due to invalid actions, and 10% due to early termination. Among the invalid actions, 44% are due to trying to remove an object from a position that does not include an object, 34% due to trying to perform an action on a separator, 10% due to trying to add an object on top of an existing one, and 2% due to trying to put an item that cannot fit in the box.

D.2 ANALYSIS OF ACTION SELECTION BIAS

We observe that the trained models often exhibit bias towards specific action arguments, which are sampled much more often than others during inference. Figure 6 illustrates this by visualizing coordinate selection frequencies on the development set for SCATTER CMDPs. While the presence

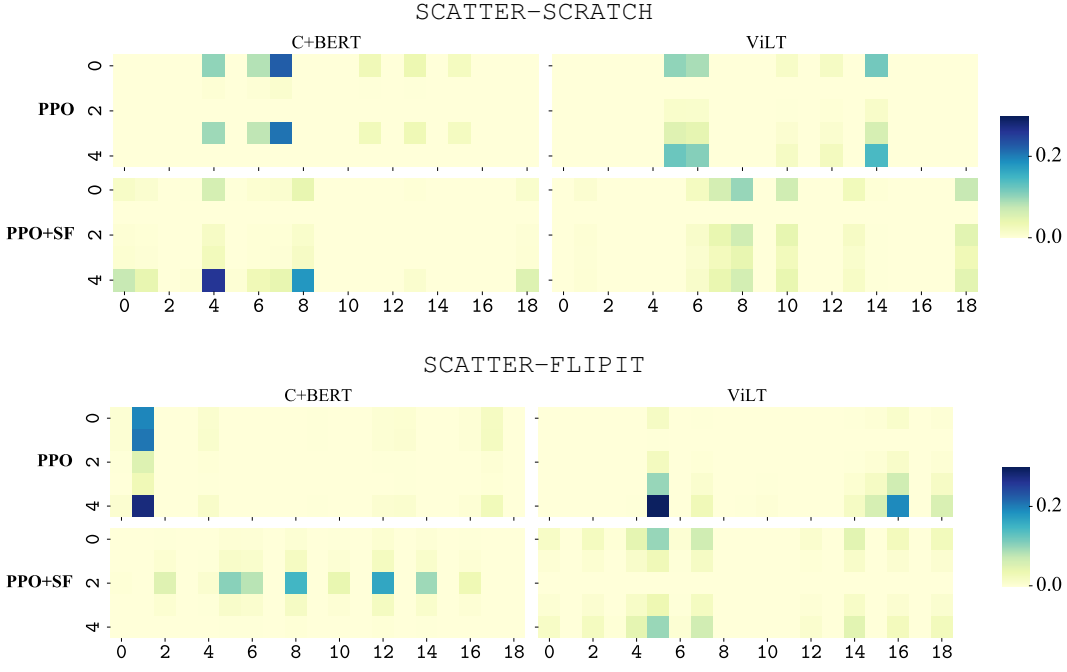


Figure 6: Frequency of selecting the grid cell (x, y) in SCATTER CMDPs for rollouts sampled on the development set. x -axis and y -axis show the x and y position of the cells in the SCATTER 19×5 grid approximation.

of bias is relatively persistent, the exact argument the models are biased towards vary. This indicates generalization limitations of our learned policies, which potentially converge to specific argument prematurely, and do not fully utilize the entire action space. We observe that this bias leads to selecting invalid actions, for example when attempting to place a large object on the edge so it crosses image boundaries.

D.3 PERFORMANCE ANALYSIS BY SEMANTIC AND SYNTACTIC PHENOMENA

Tables 5 and 6 show performance for all semantic categories identified by Suhr et al. (2017), including for categories with very few examples. We provide an example sentence for each category.

Table 5: Performance on a set of development examples annotated for semantic and syntactic categories by Suhr et al. (2017) for both models (C+BERT | ViLT) when trained with PPO. Dev performance refers to mean performance on the respective full development set. Results outperforming dev performance are in bold.

	TOWER-SCRATCH		TOWER-FLIPIT		SCATTER-SCRATCH		SCATTER-FLIPIT		Example						
	Total	Correct %	Total	Correct %	Total	Correct %	Total	Correct %							
Semantics															
Cardinality (hard)	98	67.3	78.6	480	36.7	70.8	35	31.4	37.1	119	0.0	5.0	<i>There are exactly four objects not touching any edge</i>		
Cardinality (soft)	21	81.0	85.7	82	43.9	65.9	11	9.1	18.2	42	0.0	2.4	<i>There is a box with at least one square and at least three triangles.</i>		
Existential	122	73.8	83.6	577	37.6	70.7	55	36.4	32.7	192	0.0	3.6	<i>There is a tower with yellow base.</i>		
Universal	7	14.3	14.3	28	32.1	50.0	9	44.4	55.6	36	0.0	0.0	<i>There is a black item in every box.</i>		
Coordination	19	31.6	52.6	86	29.1	70.9	15	20.0	40.0	55	0.0	0.0	<i>There are 2 blue circles and 1 blue triangle</i>		
Coreference	3	0.0	33.3	10	30.0	30.0	3	0.0	33.3	9	0.0	0.0	<i>There is a blue triangle touching the wall with its side.</i>		
Spatial Relations	93	77.4	87.1	438	39.7	69.2	39	41.0	30.8	128	0.0	5.5	<i>there is one tower with a yellow block above a yellow block</i>		
Comparative	5	40.0	20.0	20	20.0	30.0	1	100.0	100.0	4	0.0	0.0	<i>There is a box with multiple items and only one item has a different color.</i>		
Presupposition	17	47.1	58.8	74	35.1	68.9	22	40.9	40.9	78	0.0	5.1	<i>There is a box with seven items and the three black items are the same in shape.</i>		
Negation	4	75.0	75.0	15	13.3	26.7	15	33.3	28.6	53	0.0	0.0	<i>there is exactly one black triangle not touching the edge</i>		
Syntax															
Coordination	4	25.0	100.0	14	21.4	71.4	5	20.0	20.0	20	0.0	0.0	<i>There is a box with at least one square and at least three triangles.</i>		
PP Attachment	44	84.1	93.2	215	42.3	72.1	2	0.0	33.3	7	0.0	14.3	<i>There is a black block on a black block as the base of a tower with three blocks.</i>		
Dev performance	71.78		81.60		35.95		67.60		39.08		35.63		0.00		3.51

Table 6: Performance on a set of development examples annotated for semantic and syntactic categories by Suhr et al. (2017) for both models (C+BERT | ViLT) when trained with PPO+SF. Dev performance refers to mean performance on the respective full development set. Results outperforming dev performance are in bold.

	TOWER-SCRATCH		TOWER-FLIPIT		SCATTER-SCRATCH		SCATTER-FLIPIT		Example
	Total	Correct %	Total	Correct %	Total	Correct %	Total	Correct %	
Semantics									
Cardinality (hard)	98	83.7 84.7	480	24.6 62.7	35	68.6 60.0	119	6.7 22.7	<i>There are exactly four objects not touching any edge</i>
Cardinality (soft)	21	81.0 81.0	82	29.3 63.4	11	27.3 27.3	42	7.1 26.2	<i>There is a box with at least one square and at least three triangles.</i>
Existential	122	86.9 82.8	577	25.8 64.1	55	70.9 67.3	192	5.2 27.1	There is a tower with yellow base.
Universal	7	42.9 100.0	28	14.3 57.1	9	44.4 44.4	36	5.6 16.7	<i>There is a black item in every box.</i>
Coordination	19	63.2 84.2	86	34.9 60.5	15	33.3 33.3	55	3.6 14.5	<i>There are 2 blue circles and 1 blue triangle</i>
Coreference	3	33.3 66.7	10	20.0 40.0	3	33.3 66.7	9	0.0 33.3	<i>There is a blue triangle touching the wall with its side.</i>
Spatial Relations	93	83.9 84.0	438	21.0 60.3	39	82.1 76.9	128	3.9 34.4	<i>there is one tower with a yellow block above a yellow block</i>
Comparative	5	40.0 80.0	20	0.0 40.0	1	100.0 100.0	4	0.0 25.0	<i>There is a box with multiple items and only one item has a different color.</i>
Presupposition	17	58.8 94.1	74	18.9 58.1	22	68.2 72.7	78	7.7 28.2	<i>There is a box with seven items and the three black items are the same in shape.</i>
Negation	4	75.0 75.0	15	13.3 53.3	15	80.0 66.7	53	3.8 28.8	<i>there is exactly one black triangle not touching the edge</i>
Syntax									
Coordination	4	75.0 75.0	14	28.6 57.1	5	40.0 40.0	20	0.0 10.0	<i>There is a box with at least one square and at least three triangles.</i>
PP Attachment	44	95.5 84.1	215	22.8 60.0	2	0.0 0.0	7	0.0 12.5	<i>There is a black block on a black block as the base of a tower with three blocks.</i>
Dev performance	80.98 84.05		27.22 65.09		70.12 64.37		8.31 27.48		